Inorganica Chimica Acta 363 (2010) 2296–2306

Contents lists available at ScienceDirect

Inorganica Chimica Acta

journal homepage: www.elsevier.com/locate/ica

Synthesis, structure and solution chemistry of dioxidovanadium(V) complexes with a family of hydrazone ligands. Evidence of formation of centrosymmetric dimers *via* H-bonds in the solid state

Bipul Mondal [a], Michael G.B. Drew [b], Tapas Ghosh [a,*]

[a] Department of Chemistry, Ramakrishna Mission Vivekananda Centenary College, Rahara, Kolkata 700118, India
[b] Department of Chemistry, The University of Reading, PO Box 224 Whiteknights, Reading RG6 6AD, UK

ARTICLE INFO

Article history:
Received 13 January 2010
Received in revised form 16 March 2010
Accepted 19 March 2010
Available online 27 March 2010

Keywords:
Mixed-ligand oxidovanadium(V) complexes
Hydrazone complexes
Crystal structures
Hydrogen bonded centrosymmetric dimers
Reactivity

ABSTRACT

$[V^{IV}O(acac)_2]$ reacts with the methanol solution of tridentate ONO donor hydrazone ligands (H_2L^{1-4}, general abbreviation H_2L; are derived from the condensation of benzoyl hydrazine with 2-hydroxyacetophenone and its 5-substituted derivatives) in presence of neutral monodentate alkyl amine bases having stronger basicity than pyridine e.g., ethylamine, diethylamine, triethylamine and piperidine (general abbreviation B) to produce $BH^+[VO_2L]^-$ (**1**–**16**) complexes. Five of these sixteen complexes are structurally characterized revealing that the vanadium is present in the anionic part of the molecule, $[VO_2L]^-$ in a distorted square pyramidal environment. The complexes **5**, **6**, **15** and **16** containing two H-atoms associated with the amine-*N* atom in their cationic part (e.g., diethylammonium and piperidinium ion) are involved in H-bonding with a neighboring molecule resulting in the formation of centrosymmetric dimers while the complex **12** (containing only one hydrogen atom in the cationic part) exhibits normal H-bonding. The nature of the H-bonds in each of the four centrosymmetric dimeric complexes is different. These complexes have potential catalytic activity in the aerial oxidation of L-ascorbic acid and are converted into the [VO(L)(hq)] complexes containing VO^{3+} motif on reaction with equimolar amount of 8-hydroxyquinoline (Hhq) in methanol.

1. Introduction

Among the three (viz., +III, +IV and +V) physiologically important oxidation states of vanadium, the +V state has received considerable attention. The research interest on this oxidation state is largely fueled not only due to its interesting chemistry associated with its ability to exist in three different motifs viz., VO^{3+}, $V_2O_3{}^{4+}$ and $VO_2{}^+$ but also its involvement in many catalytic processes. Vanadium easily switches between the oxidation states +IV and +V and their relative stability depend upon the basicity of the coordinated ligands. The redox potential at pH 7 for the couple $H_2VO_4^- + 4H^+ + e \rightleftharpoons VO^{2+} + 3H_2O$ amounts to −0.341 V and in this range the vanadyl (VO^{2+}) is oxidized to vanadate under aerobic conditions and vanadate reduced to vanadyl by cellular components such as cysteine containing peptides (glutathione) and proteins, ascorbate, NADH and phenolic compounds [1]. The main species present under physiological aerobic conditions is the acid–base pair $H_2VO_4^- \rightleftharpoons HVO_4^{2-} + H^+$ ($pK_a = 8.1$) [2] and sufficiently strong chelating ligands are required to stabilize the cationic V^V species in solution around pH 7. The chemical similarities between vanadate and phosphate have been proposed to be responsible in explaining the mode of action in biological systems [3]. Such properties of vanadium along with its coordinative flexibility make it biologically important.

Hydrogen bonding plays significant roles in several biological processes e.g., in the regulation of metal ion reactivity as well as in the recognition and transport of various small molecules and ions [4–6], the catalytic cycle of haloperoxidase activity has been suggested to proceed through hydrogen bonding network [7–10], etc. In presence of appropriate hydrogen bonding donors, the hydrogen bonding is a general feature of vanadium(IV) and vanadium(V) complexes [11–17]. In general, these examples lead to formation of hydrogen bonded molecular assemblies ranging from simple dimers to three-dimensional networks.

Hydrazone ligands derived from the condensation of aliphatic/aromatic acid-hydrazide with aromatic 2-hydroxycarbonyl compounds are important tridentate ONO donor chelating ligands containing two intermediate basic phenolic and amide groups and one neutral imine moiety have the ability to stabilize the +V state of vanadium. As a part of our programme on the study of oxidovanadium(IV) and oxidovanadium(V) complexes with a family of benzoyl hydrazone ligands (H_2L^{1-4}, general abbreviation H_2L) it has been found that these ligands exclusively formed $[V^V{}_2O_3L_2]$

* Corresponding author. Tel.: +91 3325685674.
E-mail address: ictg_64@yahoo.co.in (T. Ghosh).

0020-1693/$ - see front matter © 2010 Elsevier B.V. All rights reserved.
doi:10.1016/j.ica.2010.03.053

complexes [18] (L^{2-} is the dianion of the tridentate hydrazone ligand) on reaction with equimolar amount of $[V^{IV}O(acac)_2]$ ($acac^-$ representing the acetylacetonate ion) in a non-hydroxylic solvent like acetone, CH_2Cl_2, $CHCl_3$, etc., while the similar reaction mixture in methanol afforded either $[V^{V}O(L)(OCH_3)]$ or $[V^{V}O(L)(OCH_3)]_2$ complexes (depending upon the substituent in the aryloxy ring of the hydrazone ligands) [19]. However, in presence of excess pyridine (py), the methanolic solution of $[V^{IV}O(acac)_2]$ and H_2L yielded the quaternary $[V^{V}O(L)(OCH_3)(py)]$ complexes [20]. This work has been done with view to studying the type of complexes formed by the reaction of equimolar mixture of $[V^{IV}O(acac)_2]$ and H_2L in presence of excess monodentate neutral amine bases having higher basicity than pyridine. In this paper we report the following findings of this work: (i) synthesis and characterization of sixteen dioxidovanadium(V)-hydrazone complexes; (ii) the solid state characterization of centrosymmetric dimers that are formed *via* H-bonding between the cationic and anionic part of the molecules of four complexes which to the best of our knowledge, is the first report of structurally characterized H-bridged centrosymmetric dimers of dioxidovanadium(V)-hydrazone complexes; (iii) catalytic activity of these complexes in the aerial oxidation of L-ascorbic acid and (iv) the transformation of these VO_2^+-complexes to the VO^{3+}-complexes at ambient condition. We have recently reported [18] the dioxidovanadium(V) complexes of the type $K(H_2O)^+[VO_2(L)]^-$ containing this family of hydrazone ligands without any structural characterization which are synthesized by the reaction of $[V_2O_3(L)_2]$ complexes with KOH in methanol. A significant number of such type of VO_2^+-complexes containing ONO donor hydrazone ligands are also available in the literature [11–15,7,18,21–25]. Such studies are important in connection with several catalytic [7–10,26–35] and medicinal [36–49] activities of vanadium complexes.

2. Experimental

2.1. Materials

$[V^{IV}O(acac)_2]$ [50] and the hydrazone ligands (H_2L^{1-4}) [51] were synthesized by the reported methods. Reagent grade solvents were dried and distilled prior to use. All other chemicals were reagent grade, obtained from commercial sources (Loba company, India) and used without further purification. Spectroscopic grade solvents were used for spectral measurements.

2.2. Synthesis of dioxidovanadium(V) complexes, (**1**–**16**)

All the sixteen (1–16) *cis*-VO_2^+ complexes containing the hydrazone ligands H_2L^{1-4} reported in this work have been synthesized by a simple general method using $[V^{IV}O(acac)_2]$ as the starting material in presence of excess monodentate alkyl amine bases like ethylamine (ea), diethylamine (dea), triethylamine (tea) and piperidine (pip).

2.2.1. $(eaH)^+[V^{V}O_2(L^1)]^-$ (**1**)

To a warm methanolic solution (20 mL) of H_2L^1 (0.254 g, 1 mmol) was added a methanolic solution (10 cm^3) of $[V^{IV}O(acac)_2]$ (0.265 g, 1 mmol) with stirring whereby a brown solution was obtained. To this brown solution a methanolic solution (10 cm^3) of ethylamine (~1 cm^3) was added with continuous stirring at room temperature. Immediately the color of the solution changed to intense yellow. This mixture was then stirred for 1 h at ~60 °C and then kept for slow evaporation at room temperature. After several days a reddish yellow crystalline product was obtained which was filtered followed by washing with methanol and dried over silica gel. Yield: 0.35 g (93%). *Anal.* Calc. for $C_{17}H_{20}N_3O_4V$: C, 53.5; H, 5.3; N, 11.0. Found: C, 53.2; H, 5.1; N, 10.9%. IR (KBr, ν_{max}/cm^{-1}): 1589 ($C{=}N_{azomethine}$), 1365 ($C{-}O_{phenolic}$), 1238 ($C{-}O_{enolate}$), 1032 (N–N), 897, 862 (V=O); 2779-3092 (N–H). Λ_M (DMF) = 58 Ω^{-1} cm^2 mol^{-1}. λ_{max} (DMSO)/nm: 386 (ε/dm^3 mol^{-1} cm^{-1} 11,235), 316 (12,400). ^1H NMR (DMSO-d_6, δ/ppm): 6.79 (brd, 1H, H-3, J = 8.0, Hz), 7.56–7.59 (m, 2H, H-4, H-13), 7.30 (brt, 1H, H-5, J = 7.8 Hz), 7.76 (brd, 1H, H-6, J = 7.8 Hz), 2.86 (s, 3H, 3 × H-8), 8.05 (dd, 2H, H-11, H-15, J = 7.6, 2.30 Hz), 7.45–7.47 (m, 2H, H-12, H-14), 2.80–2.85 (m, 2H, 2 × H-16), 1.14 (t, 3H, 3 × H-17, J = 7.3 Hz).

2.2.2. $(eaH)^+[V^{V}O_2(L^2)]^-$ (**2**)

Yield: 0.35 g (89%). *Anal.* Calc. for $C_{18}H_{22}N_3O_4V$: C, 54.7; H, 5.6; N, 10.6. Found: C, 54.4; H, 5.5; N, 10.5%. IR (KBr, ν_{max}/cm^{-1}): 1581 ($C{=}N_{azomethine}$), 1360 ($C{-}O_{phenolic}$), 1242 ($C{-}O_{enolate}$), 1032 (N–N), 933, 860 (V=O); 2712-2980 (N–H). Λ_M (DMF) = 56 Ω^{-1} cm^2 mol^{-1}. λ_{max} (DMSO)/nm: 395 (ε/dm^3 mol^{-1} cm^{-1} 9,617), 320 (12,556). ^1H NMR (DMSO-d_6, δ/ppm): 6.69 (d, 1H, H-3, J = 8.1 Hz), 7.11 (brd, 1H, H-4, J = 8.1 Hz), 2.28 (s, 3H, 5-CH_3), 7.44–7.46 (m, 2H, H-6, H-13), 2.86 (s, 3H, 3 × H-8), 8.04 (dd, 2H, H-11, H-15, J = 7.8, 2.7 Hz), 7.54–7.58 (m, 2H, H-12, H-14), 2.79-2.83 (m, 2H, 2 × H-16), 1.13 (t, 3H, 3 × H-17, J = 7.2 Hz).

2.2.3. $(eaH)^+[V^{V}O_2(L^3)]^-$ (**3**)

Yield: 0.35 g (86%). *Anal.* Calc. for $C_{18}H_{22}N_3O_5V$: C, 52.6; H, 5.4; N, 10.2. Found: C, 52.4; H, 5.3; N, 10.1%. IR (KBr, ν_{max}/cm^{-1}): 1593 ($C{=}N_{azomethine}$), 1356 ($C{-}O_{phenolic}$), 1290 ($C{-}O_{enolate}$), 1030 (N–N), 964, 932 (V=O); 3126-2804 (N–H). Λ_M (DMF) = 55 Ω^{-1} cm^2 mol^{-1}. λ_{max} (DMSO)/nm: 410 (ε/dm^3 mol^{-1} cm^{-1} 12,076), 316 (17,812). ^1H NMR (DMSO-d_6, δ/ppm): 6.75 (brd, 1H, H-3, J = 8.7 Hz), 6.97 (dd, 1H, H-4, J = 8.7, 2.7 Hz), 3.77 (s, 3H, 5-OCH_3), 7.21 (d, 1H, H-6, J = 2.7 Hz), 2.85 (s, 3H, 3 × H-8), 8.06 (brd, 2H, H-11, H-15, J = 6.6 Hz), 7.46–7.48 (m, 2H, H-12, H-14), 7.56–7.59 (m, 1H, H-13), 2.80–2.82 (m, 2H, 2 × H-16), 1.14 (t, 3H, 3 × H-17, J = 7.2 Hz).

2.2.4. $(eaH)^+[V^{V}O_2(L^4)]^-$ (**4**)

Yield: 0.39 g (94%). *Anal.* Calc. for $C_{17}H_{19}N_3O_4ClV$: C, 49.1; H, 4.6; N, 10.1. Found: C, 48.9; H, 4.5; N, 10.0%. IR (KBr, ν_{max}/cm^{-1}): 1595 ($C{=}N_{azomethine}$), 1358 ($C{-}O_{phenolic}$), 1296 ($C{-}O_{enolate}$), 1030 (N–N), 935, 874 (V=O); 2783-2991 (N–H). Λ_M (DMF) = 51 Ω^{-1} cm^2 mol^{-1}. λ_{max} (DMSO)/nm: 392 (ε/dm^3 mol^{-1} cm^{-1} 9,698), 318 (11,377). ^1H NMR (DMSO-d_6, δ/ppm): 6.81 (d, 1H, H-3, J = 8.4 Hz), 7.31 (brd, 1H, H-4, J = 8.4 Hz), 7.74 (s, 1H, H-6), 2.85 (s, 3H, 3 × H-8), 8.04–8.06 (m, 2H, H-11, H-15), 7.47–7.49 (m, 2H, H-12, H-14), 7.57–7.59 (m, 2H, H-12, H-14), 2.79-2.81 (m, 2H, 2 × H-16), 1.13 (t, 3H, 3 × H-17, J = 7.2 Hz).

2.2.5. $(deaH)^+[VO_2(L^1)]^-$ (**5**)

Yield: 0.39 g (96%). *Anal.* Calc. for $C_{19}H_{24}N_3O_4V$: C, 55.7; H, 5.9; N, 10.3. Found: C, 55.6; H, 5.7; N, 10.0%. IR (KBr, ν_{max}/cm^{-1}): 1601 ($C{=}N_{azomethine}$), 1367 ($C{-}O_{phenolic}$), 1250 ($C{-}O_{enolate}$), 1059 (N–N), 935, 897 (V=O); 2827–2988 (N–H). Λ_M (DMF) = 54 Ω^{-1} cm^2 mol^{-1}. λ_{max} (DMSO)/nm: 387 (ε/dm^3 mol^{-1} cm^{-1} 10,255), 316 (11,001). ^1H NMR (DMSO-d_6, δ/ppm): 6.77–6.83 (m, 2H, H-3, H-5), 7.29 (t, 1H, H-4, J = 7.7 Hz), 7.74 (d, 1H, H-6, J = 7.8 Hz), 2.83 (s, 3H, 3 × H-8), 8.02–8.04 (m, 2H, H-11, H-15), 7.43–7.45 (m, 3H, H-12, H-13, H-14), 2.89 (q, 4H, 2 × H-16, 2 × H-18, J = 7.2 Hz), 1.13 (t, 6H, 3 × H-17, 3 × H-19, J = 7.2 Hz).

2.2.6. $(deaH)^+[VO_2(L^2)]^-$ (**6**)

Yield: 0.40 g (94%). *Anal.* Calc. for $C_{20}H_{26}N_3O_4V$: C, 56.7; H, 6.2; N, 9.9. Found: C, 56.7; H, 6.1; N, 9.8%. IR (KBr, ν_{max}/cm^{-1}): 1582 ($C{=}N_{azomethine}$), 1358 ($C{-}O_{phenolic}$), 1244 ($C{-}O_{enolate}$), 1065 (N–N), 941, 899 (V=O); 2706–2984 (N–H). Λ_M (DMF) = 53 Ω^{-1} cm^2 mol^{-1}. λ_{max} (DMSO)/nm: 396 (ε/dm^3 mol^{-1} cm^{-1} 10,484), 320 (ε/dm^3 mol^{-1} cm^{-1} 13,094). ^1H NMR (DMSO-d_6, δ/ppm): 6.68 (d,

1H, H-3, J = 8.3 Hz), 7.11 (d, 1H, H-4, J = 8.3 Hz), 2.26 (s, 3H, 5-CH_3), 7.53 (s, 1H, H-6), 2.82 (s, 3H, 3 × H-8), 8.01–8.03 (m, 2H, H-11, H-15), 7.43-7.45 (m, 3H, H-12, H-13, H-14), 2.79–2.83 (q, 4H, 2 × H-16, 2 × H-18, J = 7.2 Hz), 1.14 (t, 6H, 3 × H-17, 3 × H-19, J = 7.2 Hz).

*2.2.7. (deaH)$^+$[$VO_2(L^3)$]$^-$ (**7**)*

Yield: 0.38 g (87%). *Anal.* Calc. for $C_{20}H_{26}N_3O_5V$: C, 54. 7; H, 6.0; N, 9.6. Found: C, 54.4; H, 5.9; N, 9.5%. IR (KBr, ν_{max}/cm^{-1}): 1587 (C=$N_{azomethine}$), 1362 (C–$O_{phenolic}$), 1275 (C–$O_{enolate}$), 1061 (N–N), 943, 895 (V=O); 2710–2984 (N–H). Λ_M (DMF) = 50 Ω^{-1} cm^2 mol^{-1}. λ_{max} (DMSO)/nm: 410 (ε/dm^3 mol^{-1} cm^{-1} 9,482), 315 (14,051). ^{1}H NMR (DMSO-d_6, δ/ppm): 6.75 (d, 1H, H-3, J = 8.9 Hz), 6.98 (dd, 1H, H-4, J = 8.9, 2.9 Hz), 3.75 (s, 3H, 5-OCH_3), 7.21 (d, 1H, H-6, J = 2.9 Hz), 2.84 (s, 3H, 3 × H-8), 8.03-8.05 (m, 2H, H-11, H-15), 7.45–7.47 (m, 3H, H-12, H-13, H-14), 2.91 (q, 4H, 2 × H-16, 2 × H-18, J = 7.3 Hz), 1.15 (t, 6H, 3 × H-17, 3 × H-19, J = 7.3 Hz).

*2.2.8. (deaH)$^+$[$VO_2(L^4)$]$^-$ (**8**)*

Yield: 0.40 g (91%). *Anal.* Calc. for $C_{19}H_{23}N_3O_4ClV$: C, 51.4; H, 5.2; N, 9.5. Found: C, 51.3; H, 5.1; N, 9.4%. IR (KBr, ν_{max}/cm^{-1}): 1595 (C=$N_{azomethine}$), 1362 (C–$O_{phenolic}$), 1240 (C–$O_{enolate}$), 1067 (N–N), 947, 920 (V=O); 2714–2986 (N–H). Λ_M (DMF) = 47 Ω^{-1} cm^2 mol^{-1}. λ_{max} (DMSO)/nm: 393 (ε/dm^3 mol^{-1} cm^{-1} 14,883), 317 (16,281). ^{1}H NMR (DMSO-d_6, δ/ppm): 6.83 (d, 1H, H-3, J = 8.8 Hz), 7.32 (dd, 1H, H-4, J = 8.8, 2.3 Hz), 7.74 (d, 1H, H-6, J = 2.3 Hz), 2.84 (s, 3H, 3 × H-8), 8.03–8.06 (m, 2H, H-11, H-15), 7.46–7.48 (m, 3H, H-12, H-13, H-14), 2.91 (q, 4H, 2 × H-16, 2 × H-18, J = 7.3 Hz), 1.15 (t, 6H, 3 × H-17, 3 × H-19, J = 7.3 Hz).

*2.2.9. (teaH)$^+$[$VO_2(L^1)$]$^-$ (**9**)*

Yield: 0.38 g (87%). *Anal.* Calc. for $C_{21}H_{28}N_3O_4V$: C, 57.7; H, 6. 5; N, 9.6. Found: C, 57.4; H, 6.4; N, 9.4%. IR (KBr, ν_{max}/cm^{-1}): 1599 (C=$N_{azomethine}$), 1367 (C–$O_{phenolic}$), 1250 (C–$O_{enolate}$), 1065 (N–N), 935, 897 (V=O); 2737–3057 (N–H). Λ_M (DMF) = 50 Ω^{-1} cm^2 mol^{-1}. λ_{max} (DMSO)/nm: 372 (ε/dm^3 mol^{-1} cm^{-1} 7,498), 308 (12,427). ^{1}H NMR ($CDCl_3$, δ/ppm): 7.02–7.07 (m, 2H, H-3, H-5), 7.36 (brd, 1H, H-4, J = 8.7 Hz), 7.72 (brd, 1H, H-6, J = 9.0 Hz), 3.00 (s, 3H, 3 × H-8), 7.73-7.76 (m, 2H, H-11, H-15), 7.65 (brd, 2H, H-12, H-14, J = 7.8 Hz), 7.19 (brd, 1H, H-13, J = 7.8 Hz), 3.46 (q, 6H, 2 × H-16, 2 × H-18, 2 × H-20, J = 7.2 Hz), 1.15 (t, 9H, 3 × H-17, 3 × H-19, 3 × H-21, J = 7.2 Hz), 9.54 (brs, 1H, N-3).

*2.2.10. (teaH)$^+$[$VO_2(L^2)$]$^-$ (**10**)*

Yield: 0.33 g (74%). *Anal.* Calc. for $C_{22}H_{30}N_3O_4V$: C, 58.5; H, 6.7; N, 9.3. Found: C, 58.4; H, 6.6; N, 9.2%. IR (KBr, ν_{max}/cm^{-1}): 1582 (C=$N_{azomethine}$), 1367 (C–$O_{phenolic}$), 1244 (C–$O_{enolate}$), 1067 (N–N), 943, 897 (V=O); 2706–2984 (N–H). Λ_M (DMF) = 48 Ω^{-1} cm^2 mol^{-1}. λ_{max} (DMSO)/nm: 384 (ε/dm^3 mol^{-1} cm^{-1} 7,569), 309 (15,680). ^{1}H NMR (DMSO-d_6, δ/ppm): 6.70 (d, 1H, H-3, J = 8.4 Hz), 7.12 (brd, 1H, H-4, J = 8.4 Hz), 2.29 (s, 3H, 5-CH_3), 7.54 (s, 1H, H-6), 2.84 (s, 3H, 3 × H-8), 8.04-8.06 (m, 2H, H-11, H-15), 7.44–7.47 (m, 3H, H-12, H-13, H-14), 2.93 (q, 6H, 2 × H-16, 2 × H-18, 2 × H-20, J = 6.9 Hz), 1.16 (t, 9H, 3 × H-17, 3 × H-19, 3 × H-21, J = 6.9 Hz).

*2.2.11. (teaH)$^+$[$VO_2(L^3)$]$^-$ (**11**)*

Yield: 0.33 g (71%). *Anal.* Calc. for $C_{22}H_{30}N_3O_5V$: C, 56.5; H, 6.5; N, 9.0. Found: C, 56.5; H, 6.3; N, 8.9%. IR (KBr, ν_{max}/cm^{-1}): 1585 (C=$N_{azomethine}$), 1363 (C–$O_{phenolic}$), 1246 (C–$O_{enolate}$), 1069 (N–N), 942, 901 (V=O); 2725–2992 (N–H). Λ_M (DMF) = 47 Ω^{-1} cm^2 mol^{-1}. λ_{max} (DMSO)/nm: 387 (ε/dm^3 mol^{-1} cm^{-1} 7,748), 312 (14,540). ^{1}H NMR ($CDCl_3$, δ/ppm): 7.00–7.04 (m, 2H, H-3, H-5), 7.32 (d, 1H, H-4, J = 8.3 Hz), 3.84 (s, 3H, 5-OCH_3), 7.25 (s, 1H, H-6), 2.98 (s, 3H, 3 × H-8), 7.72-7.75 (m, 2H, H-11, H-15), 7.64 (brd, 2H, H-12, H-14, J = 7.6 Hz), 7.20 (brd, 1H, H-13, J = 7.6 Hz), 3.45 (q, 6H, 2 × H-16, 2 × H-18, 2 × H-20, J = 7.3 Hz), 1.14 (t, 9H, 3 × H-17, 3 × H-19, 3 × H-21, J = 7.3 Hz), 10.02 (brs, 1H, N-3).

*2.2.12. (teaH)$^+$[$VO_2(L^4)$]$^-$ (**12**)*

Yield: 0.37 g (79%). *Anal.* Calc. for $C_{21}H_{27}N_3O_4ClV$: C, 53.5; H, 5.8; N, 8.9. Found: C, 53.3; H, 5.6; N, 8.8%. IR (KBr, ν_{max}/cm^{-1}): 1597 (C=$N_{azomethine}$), 1364 (C–$O_{phenolic}$), 1240 (C–$O_{enolate}$), 1072 (N–N), 953, 876 (V=O); 2592-2976 (N–H). Λ_M (DMF) = 43 Ω^{-1} cm^2 mol^{-1}. λ_{max} (DMSO)/nm: 384 (ε/dm^3 mol^{-1} cm^{-1} 7,464), 310 (13,629). ^{1}H NMR ($CDCl_3$, δ/ppm): 6.97 (d, 1H, H-3, J = 7.3 Hz), 7.38–7.42 (m, 4H, H-4, H-12, H-13, H-14), 7.70 (d, 1H, H-6, J = 2.4 Hz), 2.92 (s, 3H, 3 × H-8), 8.12–8.16 (m, 2H, H-11, H-15), 3.35 (q, 6H, 2 × H-16, 2 × H-18, 2 × H-20, J = 6.9 Hz), 1.50 (t, 9H, 3 × H-17, 3 × H-19, 3 × H-21, J = 6.9 Hz), 12.17 (brs, 1H, N-3).

*2.2.13. (pipH)$^+$[$VO_2(L^1)$]$^-$ (**13**)*

Yield: 0.34 g (81%). *Anal.* Calc. for $C_{20}H_{24}N_3O_4V$: C, 57.0; H, 5.7; N, 10.0. Found: C, 56.9; H, 5.6; N, 9.9%. IR (KBr, ν_{max}/cm^{-1}): 1592 (C=$N_{azomethine}$), 1365 (C–$O_{phenolic}$), 1251 (C–$O_{enolate}$), 1028 (N–N), 965, 891 (V=O); 2738-2955 (N–H). Λ_M (DMF) = 57 Ω^{-1} cm^2 mol^{-1}. λ_{max} (DMSO)/nm: 380 (ε/dm^3 mol^{-1} cm^{-1} 9,518), 308 (16,020). ^{1}H NMR ($CDCl_3$, δ/ppm): 7.02 (dd, 1H, H-3, J = 8.1, 0.6 Hz), 7.32–7.40 (m, 4H, H-4, H-12, H-13, H-14), 6.93 (dt, 1H, H-5, J = 7.5, 0.6 Hz), 7.78 (dd, 1H, H-6, J = 7.5, 0.8 Hz), 2.99 (s, 3H, 3 × H-8), 8.17 (dd, 2H, H-11, H-15, J = 6.5, 0.8 Hz), 3.36 (s, 4H, 2 × H-16, 2 × H-20), 1.78 (s, 4H, 2 × H-17, 2 × H-19), 1.51 (s, 2H, 2 × H-18), 9.20 (brs, 2H, 2 × N-3).

*2.2.14. (pipH)$^+$[$VO_2(L^2)$]$^-$ (**14**)*

Yield: 0.34 g (79%). *Anal.* Calc. for $C_{21}H_{26}N_3O_4V$: C, 57.9; H, 6.0; N, 9.7. Found: C, 57.8; H, 5.9; N, 9.6%. IR (KBr, ν_{max}/cm^{-1}): 1594 (C=$N_{azomethine}$), 1361 (C–$O_{phenolic}$), 1243 (C–$O_{enolate}$), 1029 (N–N), 907, 860 (V=O); 2725–2942 (N–H). Λ_M (DMF) = 55 Ω^{-1} cm^2 mol^{-1}. λ_{max} (DMSO)/nm: 386 (ε/dm^3 mol^{-1} cm^{-1} 9,202), 303 (18,173). ^{1}H NMR ($CDCl_3$, δ/ppm): 6.91 (d, 1H, H-3, J = 8.3 Hz), 7.15 (dd, 1H, H-4, J = 8.3, 0.8 Hz), 7.56 (d, 1H, H-6, J = 0.8 Hz), 2.35 (s, 3H, 5-OCH_3), 2.97 (s, 3H, 3 × H-8), 8.16 (dd, 2H, H-11, H-15, J = 6.8, 0.7 Hz), 7.37–7.42 (m, 3H, H-12, H-13, H-14), 3.36 (s, 4H, 2 × H-16, 2 × H-20), 1.79 (s, 4H, 2 × H-17, 2 × H-19), 1.53 (s, 2H, 2 × H-18).

*2.2.15. (pipH)$^+$[$VO_2(L^3)$]$^-$ (**15**)*

Yield: 0.37 g (82%). *Anal.* Calc. for $C_{21}H_{26}N_3O_5V$: C, 55.9; H, 5.8; N, 9.3. Found: C, 55.8; H, 5.7; N, 9.2%. IR (KBr, ν_{max}/cm^{-1}): 1590 (C=$N_{azomethine}$), 1360 (νC–$O_{phenolic}$), 1217 (C–$O_{enolate}$), 1032 (N–N), 952, 915 (V=O); 2714–2949 (N–H). Λ_M (DMF) = 53 Ω^{-1} cm^2 mol^{-1}. λ_{max} (DMSO)/nm: 405 (ε/dm^3 mol^{-1} cm^{-1} 8,084), 307 (10,360). ^{1}H NMR ($CDCl_3$, δ/ppm): 6.99 (s, 2H, H-3, H-4), 3.83 (s, 3H, 5-OCH_3), 7.24(s, 1H, H-6), 2.96 (s, 3H, 3 × H-8), 8.16 (d, 2H, H-11, H-15, J = 0.6 Hz), 7.40 (s, 3H, H-12, H-13, H-14), 3.34 (s, 4H, 2 × H-16, 2 × H-20), 1.81 (s, 4H, 2 × H-17, 2 × H-19), 1.55 (s, 2H, 2 × H-18), 9.25 (brs, 2H, 2 × N-3).

*2.2.16. (pipH)$^+$[$VO_2(L^4)$]$^-$ (**16**)*

Yield: 0.38 g (83%). *Anal.* Calc. for $C_{20}H_{23}N_3O_4ClV$: C, 52.7; H, 5.1; N, 9.2. Found: C, 52.5; H, 5.0; N, 9.1%. IR (KBr, ν_{max}/cm^{-1}): 1582 (C=$N_{azomethine}$), 1369 (C–$O_{phenolic}$), 1243 (C–$O_{enolate}$), 1029 (N–N), 963, 920 (V=O); 2724–2950 (N–H). Λ_M (DMF) = 49 Ω^{-1} cm^2 mol^{-1}. λ_{max} (DMSO)/nm: 388 (ε/dm^3 mol^{-1} cm^{-1} 7,349), 304 (12,867). ^{1}H NMR ($CDCl_3$, δ/ppm): 6.97 (d, 1H, H-3, J = 0.6 Hz), 7.27–7.42 (m, 4H, H-4, H-12, H-13, H-14), 7.73 (s, 1H, H-6), 2.95 (s, 3H, 3 × H-8), 8.14 (d, 2H, H-11, H-15, J = 0.6 Hz), 3.34 (s, 4H, 2 × H-16, 2 × H-20), 1.79 (s, 4H, 2 × H-17, 2 × H-19), 1.55 (s, 2H, 2 × H-18), 9.23 (brs, 2H, 2 × N-3).

2.3.1. Reaction with L-ascorbic acid

The reduction of $(eaH)^+[VO_2(L^1)]^-$ (**1**) by L-ascorbic acid was studied by electronic spectroscopy in either methanol or DMSO solution. Ascorbic acid (0.04 mmol, 14.2 mg) was added to a $(eaH)^+[VO_2(L^1)]^-$ solution (7.973×10^{-4} M, 10 mL) ($(eaH)^+[VO_2(L^1)]^-$/ascorbic ratio, molar ratio 1:10). The spectrum of the resulting solution was measured in the range 400–800 nm both before and after the addition and monitored with time until the initial spectra (i.e., before addition of ascorbic acid) was obtained. Other complexes **2**–**16** also displayed similar observation.

2.3.2. Reaction with 8-hydroxyquinoline(Hhq)

To a solution of **1** (0.10 g, 0.26 mmol) in 20 mL methanol was added Hhq (0.04 g, 0.28 mmol) dissolved 5 mL methanol. The reaction mixture was stirred at room temperature for 4 h. A deep violet solution was obtained which was kept for slow evaporation at room temperature. A shiny black microcrystalline compound was obtained after several days. The product was filtered, washed with methanol and dried over silica gel. Yield: 0.10 g (83%). This compound was found to be identical in all respect with the complex $[V^VO(L^1)(hq)]$ which was reported recently [51] from this laboratory synthesized by different method. Other complexes **2**–**16** behaved similarly.

2.4. Physical measurements

Elemental analyses were performed on a Perkin-Elmer 2400 CHNS/O analyzer. Electronic spectra (in DMSO of **1**–**12** and in CH_2Cl_2 of **13**–**16** complexes) were recorded on a Hitachi U-3501 spectrophotometer and IR spectra (as KBr pellets) were recorded on a Perkin-Elmer 782 spectrophotometer. The ^{1}H NMR spectra were recorded either in $CDCl_3$ (of **9**, **11**, **12** and **13**–**16** complexes) or in DMSO-d_6 (of **1**–**8** and **10** complexes) on a Bruker AM 300L (300 MHz) superconducting FT NMR spectrophotometer. Conductivity measurements of all the complexes were performed at 298 K in DMF solution with the Systronics 304 digital conductivity meter. The EPR spectra (X-band) of the reduced species were recorded on a E-112 Century series Varian E-102 Microwave bridge spectrometer. Tetracyanoethene (tcne) ($g = 2.0027$) was used to calibrate the EPR spectra.

2.5. Crystallographic data collection and refinement

Good quality single crystals of **5**, **6**, **12**, **15** and **16** were obtained from the respective reaction mixture upon slow evaporation of the solvent (methanol) at room temperature and they were used for structural analysis. X-ray data were measured with Mo Kα radiation at 150 K using the Oxford Diffraction X-Calibur CCD System. Data analysis was carried out with the Crysalis [52] program and the structures were solved with the SHELXS-97 program [53]. For all five structures, the non-hydrogen atoms were refined with anisotropic thermal parameters. The hydrogen atoms bonded to carbon and nitrogen were included in geometric positions and given thermal parameters equivalent to 1.2 times those of the atom to which they were attached. Absorption corrections were carried out with the ABSPACK program [54]. The structures were refined on F^2 using the SHELXL-97 program [53]. Crystallographic data are collected in Table 1.

3. Results and discussion

3.1. Synthesis

In an attempt to synthesize quaternary complexes of the type $[V^VO(L)(OCH_3)(B)]$ like $[V^VO(L)(OCH_3)(py)]$ [20] complexes with monodentate *N*-donor organic amine bases (B) having higher basicity than pyridine (py) ($pK_a = 5.48$) provides an interesting observation which encouraged as to rationalize a general synthetic method of generating dioxidovanadium(V) complexes incorporating hydrazone ligands (containing one phenolic, one enolic and one neutral imine moiety). Four monodentate neutral alkyl amine bases viz., ethylamine (ea, $pK_a = 10.64$), diethylamine (dea, $pK_a = 10.98$), triethylamine (tea, $pK_a = 10.75$) and piperidine (pip, $pK_a = 11.12$) [55], which are of higher basic than pyridine and four benzoyl hydrazone ligands (H_2L^{1-4}, Scheme 1) have been used in this study.

The dioxidovanadium(V) complexes **1**–**16** have been synthesized by the equimolar reaction of $[V^{IV}O(acac)_2]$ and H_2L in presence of B. Considering aerial oxygen being the oxidizing agent the formation of these dioxido complexes may be represented as:

$$2\left[V^{IV}O(acac)_2\right] + 2H_2L + 2B + \frac{1}{2}O_2 + H_2O \rightarrow 2BH^+\left[V^VO_2(L)\right]^- + 4Hacac, \quad (1)$$

where, Hacac is the acetylacetone.

Table 1
Crystal data and structure determination summary of the complexes **5**, **6**, **12**, **15** and **16**.

	5	6	12	15	16
Empirical formula	$C_{19}H_{24}N_3O_4V$	$C_{20}H_{26}N_3O_4V$	$C_{21}H_{27}ClN_3O_4V$	$C_{21}H_{26}N_3O_5V$	$C_{20}H_{23}N_3O_4ClV$
Formula weight	409.35	423.38	471.85	451.39	455.80
Crystal color	golden yellow	golden yellow	golden yellow	golden yellow	golden yellow
Crystal system	monoclinic	monoclinic	monoclinic	triclinic	monoclinic
Space group	$P2_1/c$	$P2_1/c$	$P2_1/n$	$P\bar{1}$	$P2_1/n$
a (Å)	8.3618(7)	8.8945(6)	13.818(2)	8.5295(9)	9.4002(5)
b (Å)	19.2985(9)	18.6042(13)	8.4821(16)	11.6703(11)	21.3238(17)
c (Å)	12.0881(10)	12.2166(8)	19.171(2)	11.9623(13)	10.0002(11)
α (°)	90	90	90	67.671(9)	90
β (°)	95.285(8)	101.235(6)	99.532(11)	85.721(9)	94.070(7)
γ (°)	90	90	90	69.120(9)	90
V (Å^3)	1942.4(2)	1982.8(2)	2215.9(6)	1026.58(18)	1999.5(3)
Z	4	4	4	2	4
$\rho_{calc.}$ (g cm^{-3})	1.400	1.418	1.414	1.460	1.514
μ (mm^{-1})	0.540	0.532	0.600	0.522	0.662
F(0 0 0)	856	888	984	472	944
Data/restraints/parameters	5590/0/247	5699/0/257	6342/0/275	4281/0/273	5719/0/263
Goodness-of-fit on F^2	0.813	1.066	0.909	0.965	0.738
R indices [$I > 2\sigma(I_0)$] R_1, wR_2	0.0466, 0.1196	0.0848, 0.2207	0.0555, 0.1351	0.0380, 0.0955	0.0548, 0.1672
R indices (all data) R_1, wR_2	0.0680, 0.1319	0.1205, 0.2346	0.0865, 0.1460	0.0558, 0.0995	0.0771, 0.1985

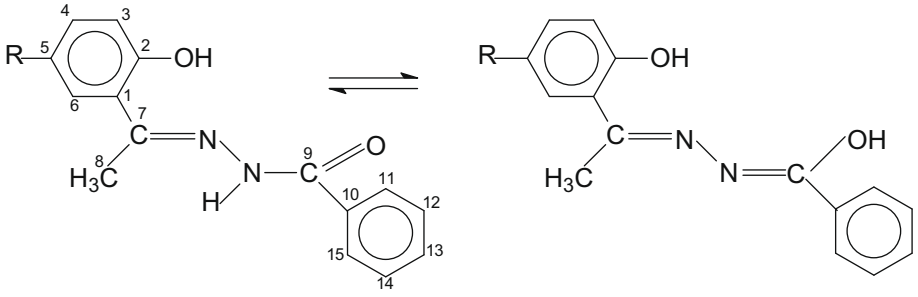

H_2L	R
H_2L^1	H
H_2L^2	CH_3
H_2L^3	OCH_3
H_2L^4	Cl

Scheme 1. Ligands employed in this study.

Similar observation was reported previously [17]. Complexes **1**-**16** are found to be diamagnetic indicating the +V state (d^0 system) of the vanadium. Molar conductance values of these dioxidovanadium(V) complexes (*vide* experimental section) in dimethylformamide (DMF) support their 1:1 electrolytic nature [56,57]. Structure determinations of five of these complexes by single crystal X-ray diffractrometry have firmly established these findings.

3.2. IR spectra of the complexes (*1* –*16*)

The tridentate dinegative mode of binding of the deprotonated hydrazone ligands with vanadium in their enol form in all these complexes is evident from the disappearance of three ligand characteristic bands [51] in the regions 1646–1651, 2924–2989, and 3215-3240 cm^{-1} due to ν(C=O), ν(N–H) and ν(O–H), respectively and the appearance of a new ν(C–O) enolate band in the 1217–1296 cm^{-1} region. The characteristic ν(C=N) and ν(N–N) stretches are observed in the 1581–1601 cm^{-1} and 1028–1072 cm^{-1} region, respectively. The shifting of ν(C=N) stretch towards the lower wave number from the free ligand [51] also supports the coordination of azomethine nitrogen [17–25,51] to the metal. The appearance of the characteristic ν(N–N) band in the appreciably higher energy region is due to diminished repulsion between the lone pairs of adjacent nitrogen atoms upon coordination. The strong band in the 1353–1369 cm^{-1} region is assigned to ν(C–O) (phenolate) [16] stretching.

In addition to these bands, all these sixteen complexes also exhibit two sharp bands in the 896–965 cm^{-1} and 829–932 cm^{-1} regions which are attributed to antisymmetric and symmetric stretching respectively of *cis*-VO_2^+ motif [16–18,21,25,58,59]. Complexes **1**–**16** exhibit a number of bands in the 2592–3157 cm^{-1} region which are assigned to the N–H stretching. The presence of multiple bands and the band width suggest that the N–H hydrogens are involved in hydrogen bonding [60,61]. Characteristic IR spectral data are collected in the experimental section.

3.3. Structure of the complexes (*5*), (*6*), (*12*), (*15*) and (*16*)

The structural analysis of five complexes reveals the following three general features: (i) both cationic and anionic parts are present in each of the molecules; (ii) vanadium is present in the anionic part of the molecule along with the coordinated hydrazone ligand while the cationic part consists of the monoprotonated form of the respective alkyl amine base and (iii) complexes **5**, **6**, **15** and **16** containing two hydrogen atoms associated with the amine nitrogen are centrosymmetric dimers which are formed *via* the intermolecular hydrogen bonding between the cationic and anionic part of the neighboring molecules (*vide infra*) while complex **12** containing one hydrogen atom linked with the amine nitrogen is monomeric exhibiting normal H-bonding between the cationic and anionic part of the molecule.

The numbering system for the five complexes is similar. So, a representative molecular structure of **5** is displayed in Fig. 1 showing the atom-numbering scheme along with the cationic and anionic part and selected bond parameters of five complexes are given in Table 2. Vanadium atom is present in the anionic part of the molecules and its coordination sphere is of the VO_4N type and the coordination geometry at the metal center can best be fitted to a distorted square pyramid with one of the two oxido oxygens at the apex. The square plane consists of a phenolic oxygen O(3), an enolic oxygen O(4) and an imine nitrogen N(1) from the fully deprotonated enolic form of the respective hydrazone ligand and the other oxido oxygen. The r.m.s. deviation of the four contributing atoms (σ) is in the range 0.008–0.212 Å (Table 3). The displacement (β) of the vanadium atom from this basal plane towards the axial oxido oxygen atom is ~0.50 Å (Table 3). The unequal bond lengths of V–O(1), V–O(2), V–O(3), V–O(4) and V–N(1) bonds as well as unequal bond angles generated by these bonds at the V-acceptor center indicate a significant distortion from the perfect square-pyramidal geometry. The amount of distortion can be quantitatively estimated from the average O(axial)–V–O/N(equatorial) angle (γ) [62] and also from τ parameter [63] (equal to Δ/60°, where Δ is the difference between the largest and next-to-largest ligand–metal–ligand angles). The average O(axial)–V–O/N(equatorial) angle and the τ parameter values are given in Table 3. For idealized square-pyramid these values are respectively 102° and zero. The deprotonated hydrazone ligands present in these five molecules form a six-membered and a five-membered chelate ring at the V(V) center with the corresponding bite angles being respectively ~81.0° and ~74.0° (exact values are collected in Table 2). The atoms in the five-membered ring are coplanar with an r.m.s. deviation (δ) of 0.022–0.071 Å (Table 3) and the six-membered ring is folded.

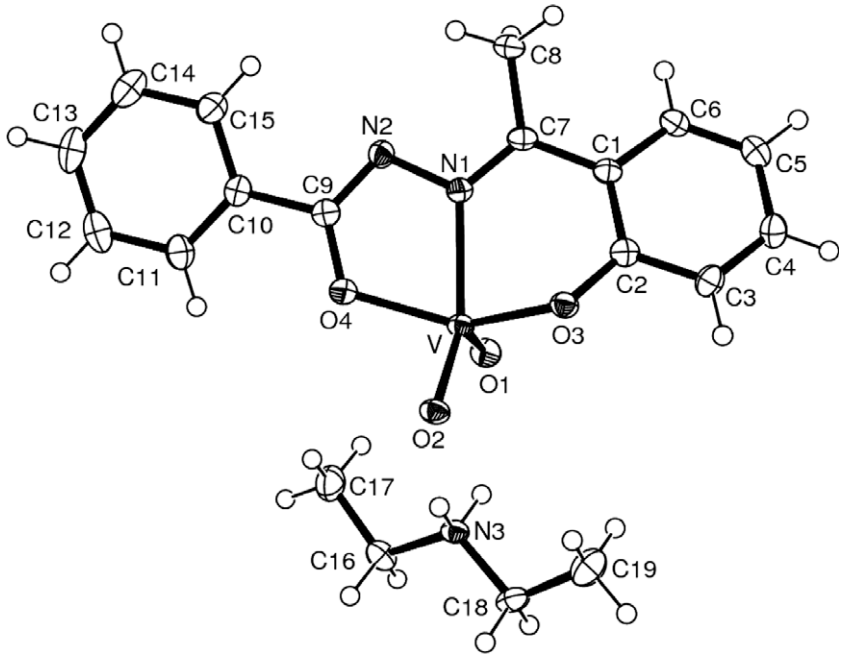

Fig. 1. ORTEP plot of complex **5** showing the atom-labeling scheme with thermal ellipsoids drawn at 50% probability level.

Table 2
Selected bond distances (Å) and angles (°) for complexes **5**, **6**, **12**, **15** and **16**.

	5	**6**	**12**	**15**	**16**
V–O(1)	1.627(1)	1.617(3)	1.607(2)	1.624(2)	1.610(2)
V–O(2)	1.643(1)	1.658(3)	1.666(2)	1.631(2)	1.645(2)
V–O(3)	1.879(1)	1.865(3)	1.883(2)	1.877(2)	1.932(2)
V–O(4)	1.958(1)	1.919(3)	1.958(2)	1.940(1)	1.969(2)
V–N(1)	2.172(2)	2.176(3)	2.181(2)	2.168(2)	2.152(2)
O(1)–V–O(2)	107.91(7)	106.54(15)	109.35(9)	109.41(10)	109.98(11)
O(1)–V–O(3)	105.82(7)	107.88(14)	105.96(8)	101.40(8)	103.32(9)
O(1)–V–O(4)	106.52(7)	103.33(14)	104.54(8)	98.62(7)	103.81(9)
O(2)–V–O(3)	96.17(6)	95.20(13)	95.34(8)	94.38(8)	94.33(9)
O(2)–V–O(4)	90.73(7)	92.62(14)	91.56(8)	94.84(7)	93.25(8)
O(3)–V–O(4)	142.93(6)	144.03(12)	144.36(8)	153.72(6)	147.30(8)
O(1)–V–N(1)	104.20(7)	102.46(14)	103.71(8)	116.06(9)	108.37(10)
O(2)–V–N(1)	147.10(7)	150.26(14)	146.35(8)	134.30(8)	141.43(9)
O(3)–V–N(1)	81.66(6)	81.88(12)	81.22(8)	81.44(6)	80.68(8)
O(4)–V–N(1)	73.28(6)	74.25(12)	74.00(7)	74.53(6)	73.71(7)
N(2)–N(1)–V	115.78(12)	113.7(2)	114.49(14)	113.75(11)	115.11(15)

Table 3
Structure characterization parameters of complexes **5**, **6**, **12**, **15** and **16**.

Complex	σ (Å)	β (Å)	γ (°)	τ	δ (Å)
5	0.008	0.523	106.1	0.069	0.022
6	0.017	0.492	105.05	0.104	0.071
12	0.015	0.523	105.9	0.033	0.047
15	0.212	0.508	106.4	0.324	0.022
16	0.082	0.530	106.4	0.098	0.065

σ = r.m.s. deviation of the four contributing atoms consisting of the square plane; β = displacement of vanadium atom from basal plane towards the axial oxido oxygen; γ = average of O(axial)–V–O/N(equatorial) angle; $\tau = \Delta/60°$, where Δ is the difference between the largest and next-to-largest ligand–metal–ligand angles; δ = r.m.s. deviation of five-membered chelate ring from co-planarity.

As shown in Fig. 2, the structure of **5** consists of a dimeric centrosymmetric unit containing two cations and anions held together with hydrogen bonds. There are two strong hydrogen bonds N(3)–H(3a)···O(1)(2 − *x*, 1 − *y*, 2 − *z*) 2.827(2) Å and N(3)–H(3b)···O(2) 2.810(2) Å. There is an additional interaction N(3)–H(3a)···O(1) of 3.004(2) Å with a N–H···O angle of 129°, while this is weaker than the former two but it is significantly stronger than the third hydrogen bond in **15** and **16** (*vide infra*). However concomitant with this is a weakening of the other hydrogen bond from H(3a), certainly as far as the subtended angle is concerned. Distances in **6** (Fig. 3) are N(3)–H(3b)···O(2)(−*x*,1 − *y*, 1 − *z*) 2.710(4) Å and N(3)–H(3a)···O(2) 2.892(4) Å. The additional weaker bond is N(3)–H(3a)···O(1) 3.048(4) Å. Thus for **6**, the hydrogen H(3a) is bifurcated, bonded to both terminal oxygen atoms O(1) and O(2) of one molecule. The dimers in **5** and **6** are different from those in **15** and **16** in that the hydrogen bonds are formed solely to the terminal oxygen atoms O(1) and O(2) and not to the phenolic oxygen atom O(3) (*vide infra*). However they differ from each other as is apparent from Figs. 2 and 3. Full dimensions for the hydrogen bonds are given in Table 4.

Fig. 4 displays the H-bonded structure of **12**. In this molecule, a significant difference in two V=O distances is observed: V–O(1) and V–O(2) are respectively 1.606(2) Å and 1.666(2) Å. The longer V–O(2) bond is probably due to its involvement in intermolecular H-bonding with the N(3)–H atom of the cationic part

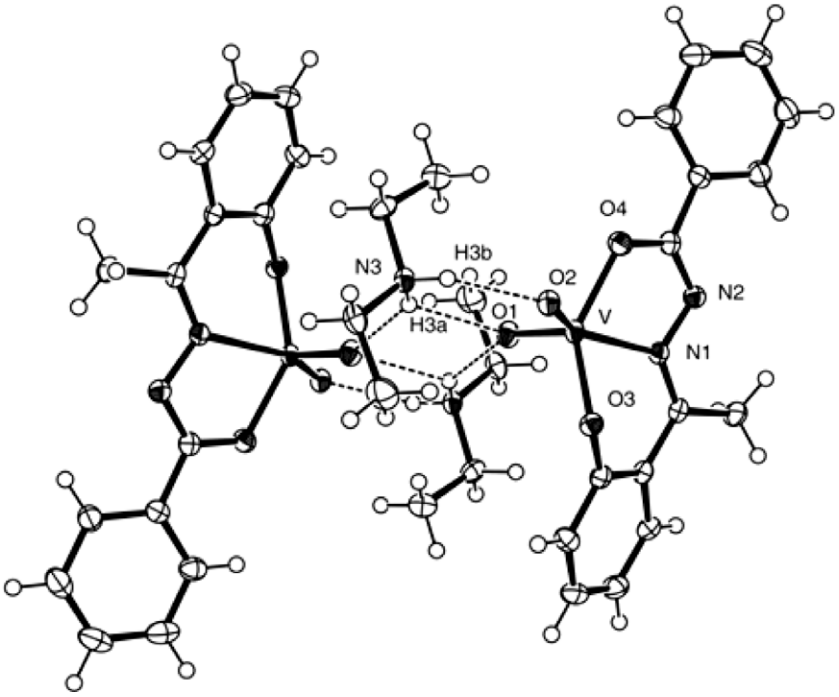

Fig. 2. The centrosymmetric dimeric structure of **5** with ellipsoids at 50% probability. Hydrogen bonds are shown as dotted lines.

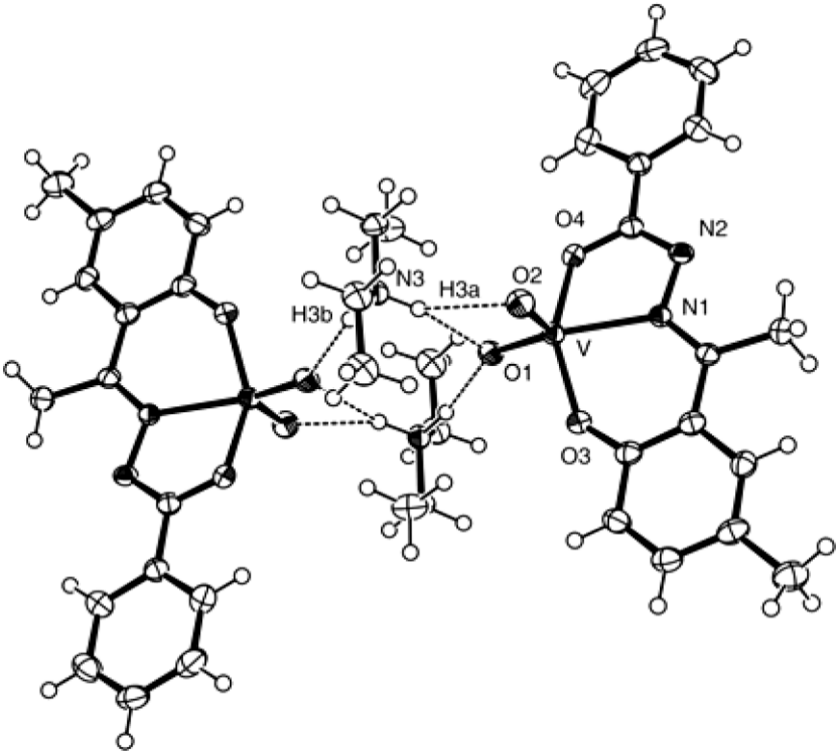

Fig. 3. The centrosymmetric dimeric structure of **6** with ellipsoids at 50% probability. Hydrogen bonds are shown as dotted lines.

(triethylammonium ion) of the molecule. The N–H···O bond distance and related details are given in Table 4. The V–O bond distances follow the order V–O(1) < V–O(2) < V–O(3) < V–O(4).

As shown in Fig. 5, the structure of **15** like **5** and **6** also consists of a dimeric centrosymmetric unit containing two cations and anions held together with hydrogen bonds. There are two strong hydrogen bonds N(3)–H(3b)···O(2) at 2.778(2) Å and N(3)–H(3a)···O(1)($-x$, $1-y$, $-z$) at 2.720(2) Å. In addition there is a weak interaction from N(3)–H(3a)···O(3) at 3.151(2) Å but with a N–H···O angle of 120°, this can represent only a weak bond. Full dimensions for the hydrogen bonds are given in Table 4. Fig. 6 displays the H-bonded dimeric structure of **16**. This structure, like **15**, also forms a centrosymmetric dimer of two cations and anions connected *via* hydrogen bonds. However in this case these involve only

Table 4
Hydrogen bond distances (Å) and bond angles (°) of complexes **5**, **6**, **12**, **15** and **16**.

Complex	D–H···A	d(H···A)	∠ DHA	d(D···A)	Symmetry element
5	N(3)–H(3a)···O(1)	2.07	141	2.827(2)	$2-x, 1-y, 2-z$
5	N(3)–H(3a)···O(1)	2.36	129	3.004(2)	
5	N(3)–H(3b)···O(2)	1.97	154	2.810(2)	
6	N(3)–H(3a)···O(2)	2.07	151	2.892(4)	
6	N(3)–H(3a)···O(1)	2.34	136	3.048(4)	
6	N(3)–H(3b)···O(2)	1.82	171	2.710(4)	$-x, 1-y, 1-z$
12	N(3)–H(3)···O(2)	1.81	175	2.718(3)	
15	N(3)–H(3b)···O(2)	1.90	166	2.778(2)	
15	N(3)–H(3a)···O(1)	1.85	162	2.720(2)	$-x, 1-y, -z$
15	N(3)–H(3b)···O(3)	2.60	120	3.151(2)	
16	N(3)–H(3a)···O(2)	1.92	152	2.749(3)	$-x, -y, 2-z$
16	N(3)–H(3b)···O(3)	2.01	156	2.861(3)	
16	N(3)–H(3a)···O(2)	2.43	116	2.941(3)	

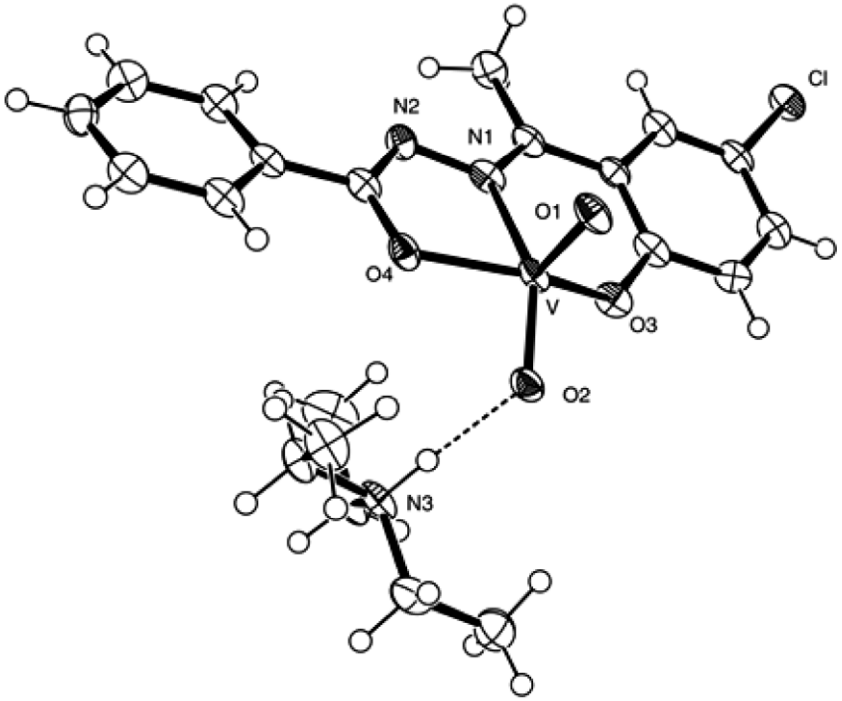

Fig. 4. The H-bonded structure of **12**.

one terminal oxygen atom O(2) together with the phenolic oxygen atom O(3) but not the second terminal oxygen atom O(1). So the dimer in **16** is completely different from that in **15** as is apparent from Fig. 5. Hydrogen bond distances are N(3)–H(3a)···O(2) ($-x$, $-y$, $2-z$) 2.749(3) Å and N(3)–H(3b)···O(3) 2.861(3) Å. There is an additional close contact N(3)–H(3a)...O(2) of 2.941(3) Å but the N–H···O angle of 116° shows this can only be a weak interaction. Full dimensions for the hydrogen bonds are given in Table 4.

Thus, while all four molecules (viz. **5**, **6**, **15** and **16**) containing two hydrogen atoms associated with the amine nitrogen in the cationic part of the respective molecule, form centrosymmetric dimers constructed from two cations and two anions but the pattern of hydrogen bonds is different in each case. In spite of best efforts, none of the four dioxidovanadium(V) complexes **1**–**4** containing the ethylammonium ion (having three hydrogen atoms available for H-bonding) in the cationic part afforded good quality single crystal suitable for structure determination by X-ray crystallography, thus giving no opportunity to study the pattern of H-bonding in these complexes.

3.4. Proton NMR spectra of the complexes

^{1}H NMR spectral data of all the complexes are given in the experimental section. The DMSO-d_6 solution of the ligands exhibits signals at $\delta \sim 11.00$ and $\delta \sim 13.00$ ppm which are attributed respectively to NH and OH protons [51]. These signals are absent in all these dioxidovanadium(V) complexes suggesting their involvement in tautomerisation of the keto form into enol form and subsequent coordination of the enolic and phenolic oxygens through deprotonation to vanadium.

Based on the IR and ^{1}H NMR spectral data, it is reasonable to assume the gross structural similarity of **1**–**4** complexes with that of **5**, **6**, **12**, **15**, and **16**.

3.5. Electronic spectra of the complexes

The electronic spectra of the complexes **1**–**12** were recorded in DMSO while that of complexes **13**–**16** in CH_2Cl_2 solution in the 300–800 nm region and the spectral data are given in the experimental section. Complexes being of d^0 system, no d–d transition

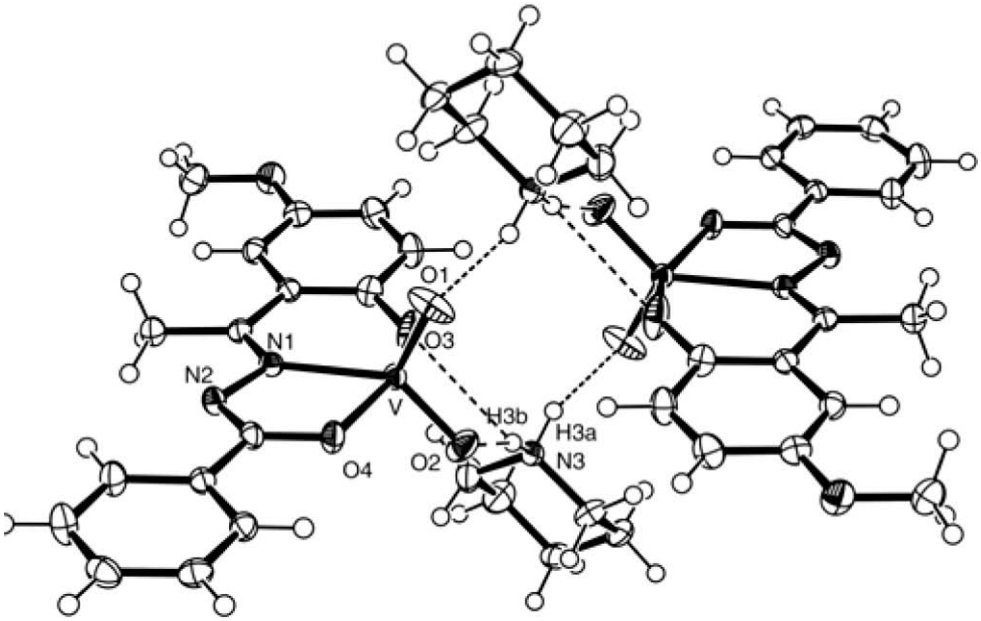

Fig. 5. The centrosymmetric dimeric structure of **15** with ellipsoids at 50% probability. Hydrogen bonds shown as dotted lines.

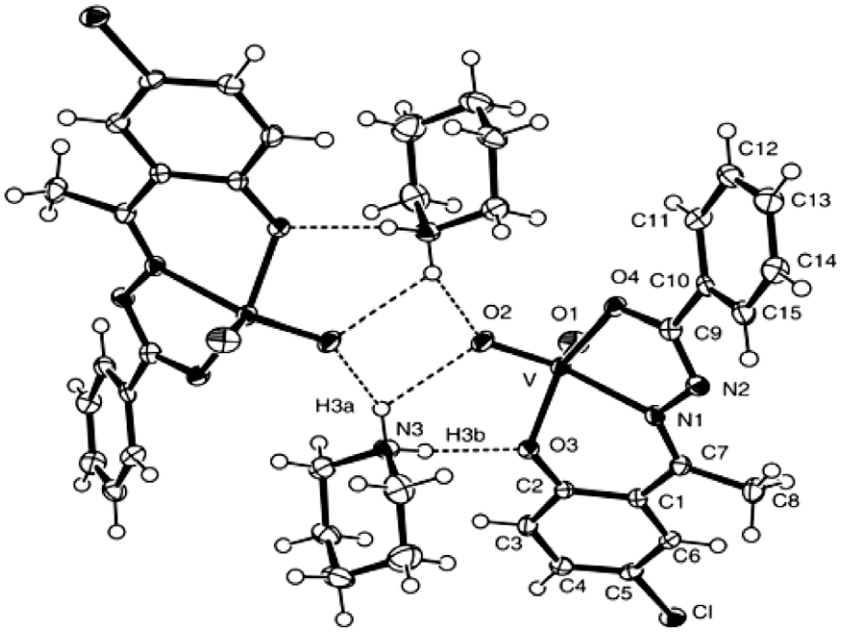

Fig. 6. The centrosymmetric dimeric structure of **16** with ellipsoids at 50% probability. Hydrogen bonds shown as dotted lines.

band is expected in their electronic spectra and in fact, all these complexes exhibit very intense transitions; the lowest energy band in the 372–410 nm region is assigned to ligand-to-metal charge transfer (LMCT) transition. The ligand characteristic $\pi \rightarrow \pi^*$ transition band of the azomethine group are observed in 308–323 nm region [18–20,25,51].

3.6. Study of the reactivity of the complexes

3.6.1. Reaction with L-ascorbic acid

The catalytic activity of these *cis*-VO_2^+ complexes (**1**–**16**) in the aerial oxidation of L-ascorbic acid has been studied in either methanol or DMSO solution. In this catalytic process, at first the vanadium(V) species is reduced by the L-ascorbic acid to vanadium(IV) which is further oxidized by the aerial oxygen to the original dioxidovanadium(V) species. The net reaction is thus an oxidation of L-ascorbic acid by atmospheric oxygen catalyzed by V(V). This reaction was monitored by ^{1}H NMR, EPR and electronic spectroscopy. These dioxidovanadium(V) complexes are yellow in color in either DMSO or CH_3OH. However, on addition of L-ascorbic acid (in excess), the yellow color immediately changed to deep green and the characteristic narrow proton signals (Supplementary Figure) of the coordinated ligand of each of the **1**–**16** complexes are converted to a broad signal which suggests that during the reaction, the $[V^VO_2(L)]^-$ complexes are reduced to a corresponding paramagnetic V^{IV} species. The absence of proton signals for the ligand strongly suggests that the ligand is still attached to the V-atom even after reduction. This green solution is EPR active

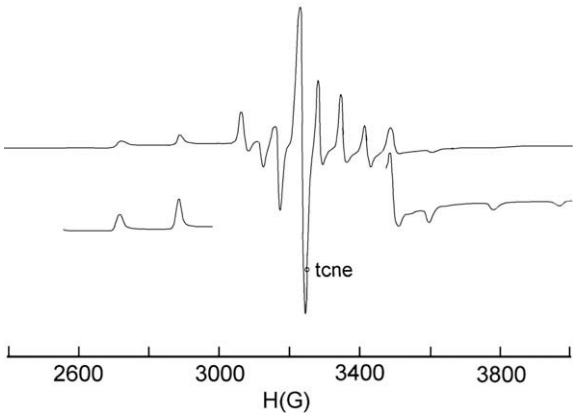

Fig. 7. X-band EPR spectra of $(deaH)^+[VO_2(L^1)]^-$, (**5**) after reduction with L-ascorbic acid in DMSO solution at 77 K; tcne = tetracyanoethene.

Table 5
EPR spectral data[a] of selected complexes after reduction with ascorbic acid at 77 K in DMSO solution.

Complex	$g_{\parallel}(10^4 A_{\parallel}/cm^{-1})$	$g_{\perp}$ $(10^4 A_{\perp}/cm^{-1})$
$(eaH)^+[VO_2(L^1)]^-$ (**1**)	1.943(170.7)	1.971(60.7)
$(deaH)^+[VO_2(L^1)]^-$ (**5**)	1.949(170.3)	1.974(60.7)
$(teaH)^+[VO_2(L^1)]^-$ (**9**)	1.945(170.5)	1.972(60.4)
$(pipH)^+[VO_2(L^1)]^-$ (**13**)	1.941(170.1)	1.971(60.6)

[a] Limits of error in g values: 0.002 and A values: 3×10^4 cm^{-1}.

and display axial EPR spectra. The EPR parameters for the first member of each of the four systems have been collected in Table 5 and a representative EPR spectra is displayed in Fig. 7. An analysis of the EPR parameter data (Table 5) reveals the relationships: $g_{\parallel} < g_{\perp}$ and $A_{\parallel} \gg A_{\perp}$, which are characteristic of an axially compressed d_{xy}^1 configuration [64–67]. Using the additivity relationship presented by Chasteen [68] and considering the reported value of different moieties [69–71], the estimated $A_{\parallel}$ value for these complexes containing one phenolic-O, one enolic-O, one imine-N and one oxido-O in the equatorial positions as revealed by the X-ray study is expected to be close to 167×10^{-4} cm^{-1} which is slightly lower than the observed value (Table 5). Such a higher observed value may be due to partial replacement of one or two coordinating sites (because the original ligand is not detached completely from the metal center as revealed by ^1H NMR spectra, *vide supra*) of the original ligand by DMSO or methanol.

Table 6
Electronic spectral data (in the 400–800 nm region) of the complexes **1**–**16** in methanol solution at 298 K after addition of L-ascorbic acid.

Complex	λ_{max} (nm) (ε/dm^3 mol^{-1} cm^{-1})
$(eaH)^+[VO_2(L^1)]^-$ (**1**)	674(375)
$(eaH)^+[VO_2(L^2)]^-$ (**2**)	679(410)
$(eaH)^+[VO_2(L^3)]^-$ (**3**)	680(391)
$(eaH)^+[VO_2(L^4)]^-$ (**4**)	674(332)
$(deaH)^+[VO_2(L^1)]^-$ (**5**)	677(363)
$(deaH)^+[VO_2(L^2)]^-$ (**6**)	678(451)
$(deaH)^+[VO_2(L^3)]^-$ (**7**)	674(361)
$(deaH)^+[VO_2(L^4)]^-$ (**8**)	677(444)
$(teaH)^+[VO_2(L^1)]^-$ (**9**)	677 (437)
$(teaH)^+[VO_2(L^2)]^-$ (**10**)	674 (344)
$(teaH)^+[VO_2(L^3)]^-$ (**11**)	674(362)
$(teaH)^+[VO_2(L^4)]^-$ (**12**)	676(349)
$(pipH)^+[VO_2(L^1)]^-$ (**13**)	676(300)
$(pipH)^+[VO_2(L^2)]^-$ (**14**)	678(376)
$(pipH)^+[VO_2(L^3)]^-$ (**15**)	678(350)
$(pipH)^+[VO_2(L^4)]^-$ (**16**)	674(228)

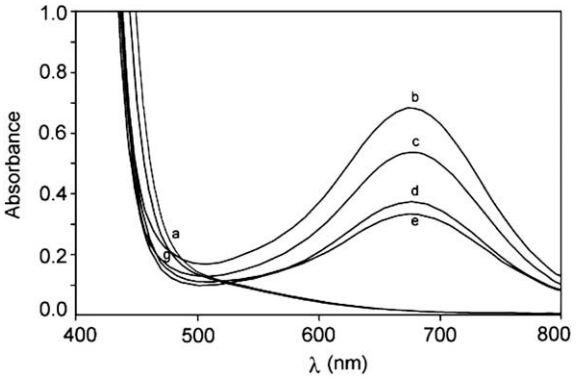

Fig. 8. Electronic spectra (400–800 nm) of a 7.973×10^{-4} mol dm^{-3} methanol solution of **5**: (a) before the addition of ascorbic acid, (b) immediately after the addition of excess (about 10 times than that of the complex) ascorbic acid, (c) 15 min after the addition of ascorbic acid, (d) 40 min after the addition of ascorbic acid, (e) 80 min after the addition of ascorbic acid and (f) 720 min after the addition of ascorbic acid.

The reversible nature of this catalytic process has been monitored by spectrophotometric study. The deep green solution obtained after the addition of L-ascorbic acid to the methanolic yellow solution of these VO_2^+ complexes exhibit a new band in the visible region near 670 nm (Table 6) which is attributed to $d_{xy} \rightarrow d_{xz}$, d_{yz} transition and the relatively large ε value indicating significant distortion in the structure. After keeping the solution in the air for sometime, the new band disappeared gradually (Fig. 8) and finally (after ~12 h) the initial spectrum was obtained indicating the re-oxidation of the reduced V^{IV}-complex to the original VO_2^+ complex thus fulfilling the criteria for a catalyst. The Scheme 2 may represent this catalytic process.

Such type of reversible redox reaction of oxidovanadium(V) complexes is very important in connection with their catalytic activity.

3.6.2. Reaction with 8-hydroxyquinoline(Hhq)

These dioxidovanadium(V) complexes are converted almost quantitatively to the monooxidovanadium(V) complexes of the

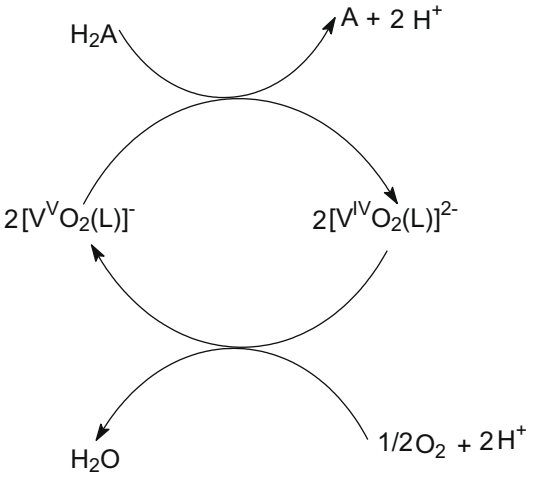

H_2A = L-Ascorbic acid; A = dehydro L-ascorbic acid

Scheme 2. Catalytic cycle for the aerial oxidation of L-ascorbic acid in presence of $[V^VO_2(L)]^-$ species.

type $[V^{V}O(L)(hq)]$ [51] (confirmed from their analytical and IR, NMR and UV–Vis spectral data) when an equimolar amount of 8-hydroxyquinoline is added to the methanolic solution of these complexes. The pH of the resulting solution is ~11 indicating the formation of base in this reaction. So, the reaction may be represented as:

$$\left[V^{V}O_2(L)\right]^{-} + Hhq \rightarrow \left[V^{V}O(L)(hq)\right] + OH^{-} \quad (2)$$

4. Conclusion

A simple general method has been established for the synthesis of *cis*-dioxidovanadium(V) complexes starting from its tetravalent precursor. Sixteen *cis*-dioxidovanadium(V) complexes have been synthesized by the equimolar reaction of $[V^{IV}O(acac)_2]$ with H_2L in presence of excess amount of alkyl amine bases (p*Ka* > 10.5). The complexes containing two hydrogen atoms attached to the amine-N atom in the cationic part of the molecules (e.g., **5**, **6**, **15** and **16**) are centrosymmetric H-bonded dimers in the solid state and the nature of H-bond is different in each of the four complexes. However, the complex containing one H-atom associated with the amine-*N* (e.g., **12**) exhibit normal H-bonding between the cationic and anionic part of the molecule. These complexes have the catalytic activity in the aerial oxidation of L-ascorbic acid. This study also indicates that these dioxidovanadium(V) complexes are easily converted to the complexes with VO^{3+} motif on reaction with a monobasic bidentate NO^{-} donor ligand (e.g., Hhq).

Acknowledgements

Our sincere thanks are due to the University Grants Commission (New Delhi, India) for financial assistance. We are thankful to our College authority for providing research facilities.

Appendix A. Supplementary material

CCDC 739922, 739923, 739924, 739925 and 739926 contain the supplementary crystallographic data for compounds **12**, **15**, **16**, **5** and **6**, respectively. These data can be obtained free of charge from The Cambridge Crystallographic Data Centre via www.ccdc.cam.ac.uk/data_request/cif. Supplementary data associated with this article can be found, in the online version, at doi:10.1016/j.ica.2010.03.053.

References

[1] D. Rehder, Inorg. Chem. Commun. 6 (2003) 604.
[2] K. Elvingson, A.G. Baró, L. Pettersson, Inorg. Chem. 35 (1996) 3388.
[3] W. Plass, Angew. Chem., Int. Ed. Engl. 38 (1999) 909.
[4] G.A. Jeffrey, W. Saenger, Hydrogen Bonding in Biological Structures, Springer, Berlin, 1991.
[5] R.H. Holm, P. Kennepohl, E.I. Solomon, Chem. Rev. 96 (1996) 2239.
[6] C. Perrin, J.B. Nielson, Ann. Rev. Phys. Chem. 48 (1997) 511.
[7] G.J. Colpas, B.J. Hamstra, J.W. Kampf, V.L. Pecoraro, J. Am. Chem. Soc. 118 (1996) 3469.
[8] A. Messerschimdt, R. Wever, Proc. Natl. Acad. Sci. USA 93 (1996) 392.
[9] M. Weyand, H.J. Hecht, M. Kieβ, M.F. Liaud, H. Vitler, D. Schomburg, J. Mol. Biol. 293 (1999) 595.
[10] M.N. Isupov, A.R. Dalby, A.A. Brindley, Y. Izumi, T. Tanabe, G.N. Murshudov, J.A. Littlechild, J. Mol. Biol. 299 (2000) 1035.
[11] W. Plass, Z. Anorg. Allg. Chem. 623 (1997) 461.
[12] W. Plass, Eur. J. Inorg. Chem. (1998) 979.
[13] W. Plass, H.P. Yozgatli, Z. Anorg. Allg. Chem. 629 (2003) 65.
[14] A. Pohlmann, W. Plass, J. Inorg. Biochem. 86 (2001) 381.
[15] A. Pohlmann, S. Nica, T.K.K. Luong, W. Plass, Inorg. Chem. Commun. 8 (2005) 289.
[16] V. Vergopoulos, W. Priebsch, M. Fritzsche, D. Rehder, Inorg. Chem. 32 (1993) 1844.
[17] M. Sutradhar, G. Mekherjee, M.G.B. Drew, S. Ghosh, Inorg. Chem. 45 (2006) 5150.
[18] B. Mondal, T. Ghosh, M. Sutradhar, G. Mukherjee, M.G.B. Drew, T. Ghosh, Polyhedron 27 (2008) 2193.
[19] B. Mondal, M.G.B. Drew, R. Banerjee, T. Ghosh, Polyhedron 27 (2008) 3197.
[20] B. Mondal, M.G.B. Drew, T. Ghosh, Inorg. Chim. Acta 362 (2009) 3303.
[21] W. Plass, A. Pohlmann, H.-P. Yozgatli, J. Inorg. Biochem. 80 (2000) 181.
[22] M.R. Maurya, S. Khurana, C. Schulzke, D. Rehder, Eur. J. Inorg. Chem. (2001) 779.
[23] M.R. Maurya, S. Khurana, W. Zhang, D. Rehder, J. Chem. Soc., Dalton Trans. (2002) 3015.
[24] M.R. Maurya, S. Agarwal, C. Bader, M. Ebel, D. Rehder, Dalton Trans. (2005) 537.
[25] T. Ghosh, Trans. Met. Chem. 31 (2006) 560.
[26] R.R. Eady, Coord. Chem. Rev. 237 (2003) 23 (and references therein).
[27] R.A. Carter-Guth, R.D. Little, A. Butler, J. Am. Chem. Soc. 125 (2003) 3688.
[28] D. Rehder, G. Santtoni, G.M. Licini, C. Schulzke, B. Meier, Coord. Chem. Rev. 237 (2003) 53.
[29] P.J. Stankicwicz, A.S. Tracy, D.C. Crans, Vanadium and its role in life, in: H. Sigel, A. Sigel (Eds.), Metal Ions in Biological Systems, vol. 31, Marcel Dekker, New York, 1995 (Chapter 9).
[30] G.L. Mendz, Arch. Biochem. Biophys. 291 (1991) 201.
[31] F. Wolff, C. Lorber, R. Choukroun, B. Donnadieu, Inorg. Chem. 42 (2003) 7839.
[32] G.W. Coates, P.D. Hustad, S. Reinartz, Angew. Chem., Int. Ed. 41 (2002) 2236.
[33] H. Hagen, J. Boersma, G. Van Koten, Chem. Soc. Rev. 31 (2002) 357.
[34] S. Gambarotta, Coord. Chem. Rev. 237 (2003) 229.
[35] C. Lorber, R. Chokroun, B. Donnadieu, Inorg. Chem. 42 (2003) 673.
[36] R. Liasko, T.A. Kabanos, S. Karkabounus, M. Malamas, J.A. Tasiopoulos, D. Stefanou, P. Collery, A. Evangelou, Anticancer Res. 18 (1998) 3609.
[37] A. Evangelou, Crit. Rev. Oncol. Hematol. 42 (2002) 249.
[38] H. Sakurai, K. Tsuchiya, M. Nakatsuka, J. Kawada, S. Ishikawa, H. Yoshida, M. Komatsu, J. Clin. Biochem. Nutr. 8 (1990) 193.
[39] J.H. McNeill, V.G. Yuen, H.R. Hoveyda, C. Orvig, J. Med. Chem. 35 (1992) 1489.
[40] P. Caravan, L. Gelmini, N. Glover, F.G. Herring, H. Li, J.H. McNeill, S.J. Retting, I.A. Setyawati, E. Shuter, Y. Sun, A.S. Tracey, V.G. Yuen, C. Orvig, J. Am. Chem. Soc. 117 (1995) 12759.
[41] D.C. Crans, M. Mahroof-Tahir, P.K. Shin, A.D. Keramidas, Mol. Cell. Biochem. 153 (1995) 17.
[42] K.H. Thomson, C. Orvig, Coord. Chem. Rev. 219–221 (2001) 1033.
[43] H. Sakurai, Y. Kojima, Y. Yoshikawa, K. Kawabe, H. Yasui, Coord. Chem. Rev. 226 (2002) 187.
[44] S.A. Dikanov, B.D. Liboiron, C. Orvig, J. Am. Chem. Soc. 124 (2002) 2969.
[45] B. Song, N. Aebischer, C. Orvig, Inorg. Chem. 41 (2002) 1357.
[46] D. Rehder, J.C. Pessoa, C.F. Geraldes, J. Biol. Inorg. Chem. 7 (2002) 675.
[47] D.C. Crans, L. Yang, J.A. Alfano, L.H. Chi, W. Jin, M. Mahroof-Tahir, K. Robbins, M.M. Toloue, L.K. Chan, A.J. Plante, R.Z. Grayson, G.R. Willsky, Coord. Chem. Rev. 237 (2003) 13.
[48] H. Sakurai, T. Goda, S. Shimomura, Biochem. Biophys. Res. Commun. 107 (1982) 1349.
[49] O.J. D' Cruz, P. Ghosh, F.M. Uckun, Biol. Reprod. 58 (1998) 1515.
[50] R.A. Rowe, M.M. Jones, Inorg. Synth. 5 (1957) 113.
[51] T. Ghosh, B. Mondal, T. Ghosh, M. Sutradhar, G. Mukherjee, M.G.B. Drew, Inorg. Chim. Acta 360 (2007) 1753.
[52] Crysalis Program, Oxford Diffraction Ltd., 2005.
[53] G.M. Sheldrick, SHELXS-97 and SHELXL-97 Programs for Crystallography Structure Solution and Refinement, University of Göttingen, Germany, 1997.
[54] ABSPACK Program, Oxford Diffraction Ltd., 2005
[55] D.D. Perrin, IUPAC Stability Constant of Metal-ion Complexes: Part B, Organic Ligands, 1st ed., Pergamon Press, Oxford, UK, 1979.
[56] J.E. Huheey, E.A. Keiter, R.L. Keiter, Inorganic Chemistry Principles of Structures and Reactivity, fourth ed., Harper Collins College Publishers, New York, 1993, p. 389.
[57] W.J. Geary, Coord. Chem. Rev. 7 (1971) 81.
[58] S. Dutta, P. Basu, A. Chakravorty, Inorg. Chem. 32 (1993) 5343.
[59] G. Asgedom, A. Sreedhara, J. Kivikoski, J. Valkonen, E. Kolehmainen, C.P. Rao, Inorg. Chem. 35 (1996) 5674.
[60] T. Steiner, Angew. Chem., Int. Ed. 41 (2002) 48.
[61] S. Pal, S. Pal, Eur. J. Inorg. Chem. (2003) 4244.
[62] E.L. Muetterties, L.J. Guggenberger, J. Am. Chem. Soc. 96 (1974) 1748.
[63] A.W. Addison, T.N. Rao, J. Reedjik, J. van Rijn, G.C. Verschoor, J. Chem. Soc., Dalton Trans. (1984) 1349.
[64] G.R. Hanson, T.A. Kabanos, A.D. Keramidas, D. Mentzafos, A. Terzis, Inorg. Chem. 31 (1992) 2587.
[65] J. Chakravarty, S. Dutta, A. Dey, A. Chakravorty, J. Chem. Soc., Dalton Trans. (1994) 557.
[66] T. Ghosh, S. Bhattacharya, A. Das, G. Mukherjee, M.G.B. Drew, Inorg. Chim. Acta 358 (2005) 989.
[67] T. Ghosh, B. Mondal, J. Chem. Res. (2007) 407.
[68] N.D. Chasteen, in: J. Lawrence, L.J. Berliner, J. Reuben (Eds.), Biological Magnetic Resonance, vol. 3, Plenum, New York, 1981, p. 53.
[69] T.S. Smith II., C.A. Root, J.W. Kampf, P.G. Rasmussen, V.L. Pecoraro, J. Am. Chem. Soc. 122 (2000) 767.
[70] E.J. Tollis, V.I. Teberekidis, C.P. Raptopoulou, A. Terzis, M.P. Sigalas, Y. Deligiannakis, T.A. Kabanos, Chem. Eur. J. 7 (2001) 2698.
[71] A. Dörnyei, S. Marcão, J.C. Pessoa, T. Jakuschi, T. Kiss, Eur. J. Inorg. Chem. (2006) 3614.